
Climate Data Record (CDR) Program

Climate Algorithm Theoretical Basis Document (C-ATBD)

Outgoing Longwave Radiation – Monthly



CDR Program Document Number: CDRP-ATBD-0097
Configuration Item Number: 01B-06
Revision 4 October 01, 2017

A controlled copy of this document is maintained in the CDR Program Library.
Approved for public release. Distribution is unlimited.

REVISION HISTORY

Rev.	Author	DSR No.	Description	Date
1	Hai-Tien Lee, CICS/UMD	DSR-102	Initial submission to CDR Program	09/01/2011
2	Hai-Tien Lee, CICS/UMD	DSR-586	Change made per CDRP-CR-0011	12/16/2013
3	Hai-Tien Lee, CICS/UMD	DSR-597	Change made per CDRP-CR-0029	01/03/2014
4	Hai-Tien Lee, CICS/UMD	DSR-1210	Update/revisions for v02r07 (includes major algorithm revisions and software rejuvenation) CR-0054	10/01/2017

TABLE of CONTENTS

1. INTRODUCTION	7
1.1 Purpose	7
1.2 Definitions	7
1.3 Referencing this Document.....	8
1.4 Document Maintenance	8
2. OBSERVING SYSTEMS OVERVIEW	9
2.1 Products Generated	9
2.2 Instrument Characteristics.....	9
3. ALGORITHM DESCRIPTION	14
3.1 Algorithm Overview.....	14
3.2 Processing Outline	14
3.3 Algorithm Input	16
3.3.1 Primary Sensor Data	16
3.3.2 Ancillary Data.....	16
3.3.3 Derived Data	19
3.3.4 Forward Models	19
3.4 Theoretical Description.....	19
3.4.1 Physical and Mathematical Description	20
3.4.2 Data Merging Strategy.....	22
3.4.3 Numerical Strategy	22
3.4.4 Calculations	22
3.4.5 Look-Up Table Description	24
3.4.6 Parameterization	25
3.4.7 Algorithm Output	25
4. TEST DATASETS AND OUTPUTS	26
4.1 Test Input Datasets.....	26
4.2 Test Output Analysis.....	26
4.2.1 Reproducibility	26
4.2.2 Precision and Accuracy.....	27
4.2.3 Error Budget	32
5. PRACTICAL CONSIDERATIONS	33
5.1 Numerical Computation Considerations	33
5.2 Programming and Procedural Considerations.....	33
5.3 Quality Assessment and Diagnostics	33
5.4 Exception Handling	33
5.5 Algorithm Validation.....	34
5.6 Processing Environment and Resources.....	35
6. ASSUMPTIONS AND LIMITATIONS	36

6.1	Algorithm Performance	36
6.2	Sensor Performance.....	37
7.	FUTURE ENHANCEMENTS.....	38
7.1	Enhancement 1 - OLR Model for IASI and CrIS	38
7.2	Enhancement 2 - OLR Regression Model.....	38
7.3	Enhancement 3 - Intersatellite Calibration.....	38
7.4	Enhancement 4 - Radiance Calibration.....	38
7.5	Enhancement 5 - Limb darkening error.....	39
8.	REFERENCES.....	40
	APPENDIX A. ACRONYMS AND ABBREVIATIONS.....	42
	APPENDIX B. MONTHLY OLR CDR V02R07 REVISIONS	43

LIST of FIGURES

Figure 1	Equator crossing times for the ascending orbit of the NOAA POES and MetOp satellites. Refer Table 2.3 for the satellite ID labels.....	13
Figure 2	HIRS OLR CDR production system overview.....	15
Figure 3	HIRS OLR CDR production flow chart.....	16
Figure 4	TOA upward longwave radiation spectrum for standard mid-latitude summer case. The smooth curves are the Planck function evaluated at 200°K, 250°K and 294°K (surface temperature for this case), respectively for reference purpose.	21
Figure 5	Differences of Global mean OLR CDR between the Rejuvenated and the baseline version of the v02r07 code packages. (Rejuvenated version is labeled as “Pack5d”).....	27
Figure 6	Similar to Figure 5 but is for the standard deviation of the global monthly mean OLR differences.....	27
Figure 7	Time series of the global mean monthly OLR, OLR CDR minus EBAF. (Blue: OLR CDR v02r02-1; Red: v02r07) The smaller disagreement in the annual cycle discrepancies is an evidence of the improvements in v02r07. Note that the EBAF Ed.4 OLR has been adjusted upwards by an about 0.5 Wm ⁻² relative to Ed2.8. The trended differences between 2000-2003 are related to the relatively larger uncertainties in the EBAF data that was constructed with TERRA CERES observations only.	28
Figure 8	Similar to Figure 7 but for the standard deviation. The OLR CDR v02r07 has improved significantly in both the annual cycle amplitude as well the spatial distribution, relative to the EBAF Ed4 data. The standard deviation of the regional differences in the two products is below 2 Wm ⁻² .	

The spikes shown in the earlier period and one near 2014 are due to the sampling differences, mostly due to the missing data in MODIS that prevents CERES from generating products..... 28

Figure 9 Similar to Figure 7 but for the RMS differences. The OLR CDR v02r07 has improved the overall agreement of the spatial distribution, relative to the EBAF Ed4 data. The RMS of the regional differences in the two products is at about 2.5 Wm^{-2} level..... 29

Figure 10 Averaged regional OLR differences between OLR CDR v02r07 and EBAF Ed4, over the period of March 2000 to Dec 2016. Two profound geographical features can be identified: a) desert areas over the North Africa; b) sub-tropical, especially near the eastern Pacific Ocean. These are the problems for future improvements. 29

Figure 11 Averaged regional OLR differences between OLR CDR v02r07 and EBAF Ed4, over the period of March 2000 to Dec 2016. Two profound geographical features can be identified: a) desert areas over the North Africa; b) sub-tropical, especially near the eastern Pacific Ocean. These are the problems for future improvements. 30

Figure 12 Similar to Figure 11 but is for the Standard deviation of the OLR differences. The largest random errors were found in the western Pacific warm pool and over the Antarctica. 30

Figure 18 Similar to Figure 11 but is for the RMS differences. The relatively larger discrepancies were found over the eastern tropical Pacific Ocean, Sahara deserts, and the eastern Antarctica..... 31

Figure 14 Description of HIRS instrument variations. 43

Figure 15 Illustration of consistency issues in OLR retrievals and the improvements made with new regression model. 44

Figure 16 Comparison Tropical and Global OLR Anomalies of OLR CDR products (Monthly v2.2, v2.7 and Daily v1.2)..... 45

Figure 17 Comparison of OLR CDR (Monthly v2.2, v2.7 and Daily v1.2) products against CERES EBAF v2.6r OLR product..... 46

Figure 18 Comparison of OLR CDR (Monthly v2.2, and Daily v1.2) products with Reanalysis data sets, CFSR, ERA-Interim and MERRA..... 46

LIST of TABLES

Table 1 Versions of the HIRS OLR CDR product release, the corresponding software package, and the CATBD..... 8

Table 2 Description of instrument parameters for variant versions of HIRS instruments with an assumed satellite altitude of 833 km..... 10

Table 3 Description of HIRS channel spectral locations and sensing properties. The channels that are used by OLR algorithm are shown. Note that the OLR retrieving channels for HIRS/3 and 4 are different from those of HIRS/2.	11
Table 4 Description of HIRS instrument type and Level-1b data set coverage available for the HIRS OLR CDR production.	12
Table 5 OLR Intersatellite Bias Adjustments, in unit Wm^{-2}	18
Table 6 Error sources and best estimated magnitude for HIRS OLR CDR production.....	32

1. Introduction

1.1 Purpose

The purpose of this document is to describe the HIRS Outgoing Longwave Radiation (OLR) Climate Data Record (CDR) algorithm and software package. The HIRS OLR CDR algorithm estimates the OLR with the radiance observations from the High Resolution Infrared Radiation Sounder (HIRS) instruments onboard TIROS-N series and MetOp polar orbiters and generates the continuous OLR time series as gridded global maps from 1979 to the present. The explanations of the algorithm and the software package provide a guide to the understanding of algorithm theoretical basis and performance, as well the product generation procedures.

1.2 Definitions

Following is a summary of the symbols used to define the algorithm.

Spectral and directional parameters:

λ = wavelength (μm)

ν = wavenumber (cm^{-1})

θ = view zenith angle or local zenith angle (degree)

φ = relative azimuth angle (degree)

$I_{\nu}^{\uparrow}(z, \theta, \varphi)$ = upward specific intensity at height z ($\text{Wm}^{-2} \text{sr}^{-1} (\text{cm}^{-1})^{-1}$)

$\Phi_i(\nu)$ = normalized spectral response function for the i^{th} channel (unit-less)

$N_i(\theta, \varphi)$ = TOA radiance observed from satellite for the i^{th} channel ($\text{Wm}^{-2} \text{sr}^{-1} (\text{cm}^{-1})^{-1}$)

$N_{\Delta\nu}(\theta, \varphi)$ = TOA radiance integrated over wavenumber interval $\Delta\nu$ ($\text{Wm}^{-2} \text{sr}^{-1}$)

$F^{\uparrow}(z, \theta, \varphi)$ = upward radiant flux intensity at height z ($\text{Wm}^{-2} \text{sr}^{-1}$)

$F_{\nu}^{\uparrow}(z)$ = upward spectral flux at height z ($\text{Wm}^{-2} (\text{cm}^{-1})^{-1}$)

$F^{\uparrow}(z)$ = upward flux (cf. radiant flux density, or irradiance) at height z (Wm^{-2})

$B_{\nu}(T)$ = Planck function evaluated at wavenumber ν at a temperature T ($\text{Wm}^{-2} \text{sr}^{-1} (\text{cm}^{-1})^{-1}$)

C_1 = First Planck function coefficient ($\text{Wm}^{-2} \text{sr}^{-1} (\text{cm}^{-1})^{-1} (\text{cm}^{-1})^{-3}$)

C_2 = Second Planck function coefficient ($(\text{cm}^{-1})^{-1}$ Kelvin)

Atmospheric parameters:

$$\tau_{\nu}(z, \theta) = \text{optical depth (unit-less)}$$

1.3 Referencing this Document

This document should be referenced as follows:

Outgoing Longwave Radiation - Monthly - Climate Algorithm Theoretical Basis Document, NOAA Climate Data Record Program CDRP-ATBD-0097 Rev. 4 (2017). Available at <http://www.ncdc.noaa.gov/cdr/operationalcdrs.html>

1.4 Document Maintenance

Table 1.1 defines the versions of the HIRS OLR CDR product release, the corresponding software package, and the CATBD. The Production software package is maintained at NCDC Subversion version control system.

Table 1 Versions of the HIRS OLR CDR product release, the corresponding software package, and the CATBD

Release Date	Product Version	Software Version	CATBD Version	Subversion Branch	Remarks
2011-09-01	V02R02	V02R02	v1.0		Initial Release
2017-10-01	V02R07	V02R07	v4.0		Upgrade revision

2. Observing Systems Overview

2.1 Products Generated

The product generated is the monthly mean OLR time series in 2.5°x2.5° equal-angle gridded global maps spanning from January 1979 to the present (and continues on). The OLR is estimated from the HIRS radiance observations directly, for all sky conditions. The HIRS instruments are flown onboard the NOAA TIROS-N series and Eumetsat MetOp-A (and B) operational polar-orbiting satellites.

OLR is one of the three components that determine the TOA earth radiation budget. OLR has been extensively used in the investigations of the cloud/water vapor/radiative interaction processes, climate variability, and for climate change monitoring and numerical model evaluation and diagnostics, etc. It has also been used to estimate large-scale precipitation. OLR is identified as one of the “Essential Climate Variables” in WMO Global Climate Observing System (GCOS).

2.2 Instrument Characteristics

HIRS is one of the three sounding instruments that constitute the TIROS Operational Vertical Sounder (TOVS, and later becomes Advanced TOVS, ATOVS) system onboard the NOAA TIROS-N series and Eumetsat MetOp-A/B satellites. The detailed description of HIRS instrument characteristics, Level-1b data format, the TOVS system, and the system configurations for the NOAA TIROS-N series polar orbiters can be found in the NOAA Polar Orbiter Data (POD) User's Guide (1998 version) and NOAA KLM User's Guide (2009 version).

There are some relatively minor variations in HIRS instrument design. Table 2.1 lists the HIRS instrument parameters for the variant versions (cf. NOAA POD User's Guide Table 4.0-1; NOAA KLM User's Guide Section 3.2.2 and Appendix J). It's noteworthy to point out that the onboard warm target calibration reference has been changed from two blackbodies in HIRS/2 and 2I to one blackbody in HIRS/3 and 4. The HIRS/4 FOV resolution is enhanced to 10 km, which is about twice better than the earlier HIRS versions.

Table 2 Description of instrument parameters for variant versions of HIRS instruments with an assumed satellite altitude of 833 km

Parameters	HIRS/2	HIRS/2I	HIRS/3	HIRS/4
Calibration	Two Stable blackbodies and space background	Two Stable blackbodies and space background	One Stable blackbody (290K) and space background	One Stable blackbody (286K) and space background
Cross-track scan angle (degrees from nadir)	± 49.5	± 49.5	± 49.5	± 49.5
Scan time (seconds)	6.4	6.4	6.4	6.4
Number of steps	56	56	56	56
Angular FOV (degrees)	1.22	1.40	1.40 (Ch1-12) 1.3 (Ch13-19)	0.69
Step angle (degrees)	1.8	1.8	1.8	1.8
Step time (seconds)	0.1	0.1	0.1	0.1
Ground IFOV at nadir (km diameter)	17.4	20.4	20.3 (Ch1-12) 18.9 (Ch13-19)	10
Ground IFOV at end of scan	58.5 km cross-track x 29.9 km along-track	68.3 km cross-track x 34.8 km along-track	68.3 km cross-track x 34.8 km along-track	34.2 km cross-track x 17.4 km along-track
Distance between IFOV centers (km along-track)	42.0	42.0	42	42
Swath width	± 1120 km	± 1124 km	± 1124 km	± 1107 km
Data precision (bits)	13	13	13	13

HIRS consists of nineteen infrared channels (channels 1-19) and one visible channel (channel 20). Table 2.2 lists the central wavenumbers and the sensing properties for the HIRS/2 on NOAA-9 as an example, with the channels used in HIRS OLR algorithm indicated. Specifications for HIRS/3 and 4 are available on NOAA KLM User's Guide.

Table 3 Description of HIRS channel spectral locations and sensing properties. The channels that are used by OLR algorithm are shown. Note that the OLR retrieving channels for HIRS/3 and 4 are different from those of HIRS/2.

Channel	Central wavenumber (cm ⁻¹)	Used in HIRS/2 OLR Algorithm	Sensing Properties
1	667.67		15 μm CO ₂ band
2	679.84		15 μm CO ₂ band
3	691.46	✓	15 μm CO ₂ band
4	703.37		15 μm CO ₂ band
5	717.16		15 μm CO ₂ band
6	732.64		15 μm CO ₂ band
7	749.48	✓	15 μm CO ₂ band
8	898.53	✓	Window
9	1031.61		Ozone
10	1224.74		Water Vapor
11	1365.12	✓	Water Vapor
12	1483.24	✓	Water Vapor
13	2189.97		4.3 μm CO ₂ band
14	2209.18		4.3 μm CO ₂ band
15	2243.14		4.3 μm CO ₂ band
16	2276.46		4.3 μm CO ₂ band
17	2359.05		4.3 μm CO ₂ band
18	2518.14		Window
19	2667.80		Window
20	14549.27		Visible Window

Table 2.3 describes the HIRS instrument types and the availability of HIRS Level-1B data. The near real-time instrument health condition is available at NESDIS POES Status Monitoring website (<http://www.oso.noaa.gov/poesstatus/> as of July 18, 2011). The satellite ID is the code name for these polar orbiters that will be referred in the HIRS OLR CDR production package and in this document henceforth.

Errata: The Note 7 of Table J.1 on KLM User's Guide Appendix J states that "HIRS/2I was flown on NOAA-14 only". This statement is incorrect. HIRS/2I instruments were flown on both NOAA-11 and 14.

Table 4 Description of HIRS instrument type and Level-1b data set coverage available for the HIRS OLR CDR production.

Satellite	Satellite ID	Data coverage	Instrument Type
TIROS-N (TN)	N05	1978 d294 – 1980 d054	HIRS/2
NOAA-6 (NA)	N06	1979 d181 – 1983 d064 1985 d098 – 1985 d181 1985 d290 – 1986 d319	HIRS/2
NOAA-7 (NC)	N07	1981 d236 – 1985 d032	HIRS/2
NOAA-8 (NE)	N08	1983 d123 – 1984 d163 1985 d182 – 1985 d287	HIRS/2
NOAA-9 (NF)	N09	1984 d348 – 1988 d312	HIRS/2
NOAA-10 (NG)	N10	1986 d329 – 1991 d259	HIRS/2
NOAA-11 (NH)	N11	1988 d313 – 1995 d100 1997 d196 – 2000 d117	HIRS/2I
NOAA-12 (ND)	N12	1991 d259 – 1998 d348	HIRS/2
NOAA-14 (NJ)	N14	1995 d001 – 2006 d283	HIRS/2I
NOAA-15 (NK)	N15	1998 d299 – 2009 d120	HIRS/3
NOAA-16 (NL)	N16	2001 d001 – 2014 d165	HIRS/3
NOAA-17 (NM)	N17	2002 d191 – 2013 d099	HIRS/3
NOAA-18 (NN)	N18	2005 d156 – present	HIRS/4
NOAA-19 (NP)	N19	2009 d153 – present	HIRS/4
MetOp-A (M2)	N20	2006 d325 – present	HIRS/4
MetOp-B (M1)	N21	2013 d015 – present	HIRS/4

NOAA POES were historically configured to fly with one morning and one afternoon satellites, nominally at 7:30 and 2:30 equator crossing time, respectively. The polar-orbiter configuration was changed since NOAA-17, which was moved to the late morning 10:30 orbit. Since they are all in precessing orbits, their equator crossing times change slowly corresponding to the orbital drifts. Figure 1 describes the equator crossing times of the NOAA POES and MetOp satellites in their course of operation, for the ascending branch of the orbits.

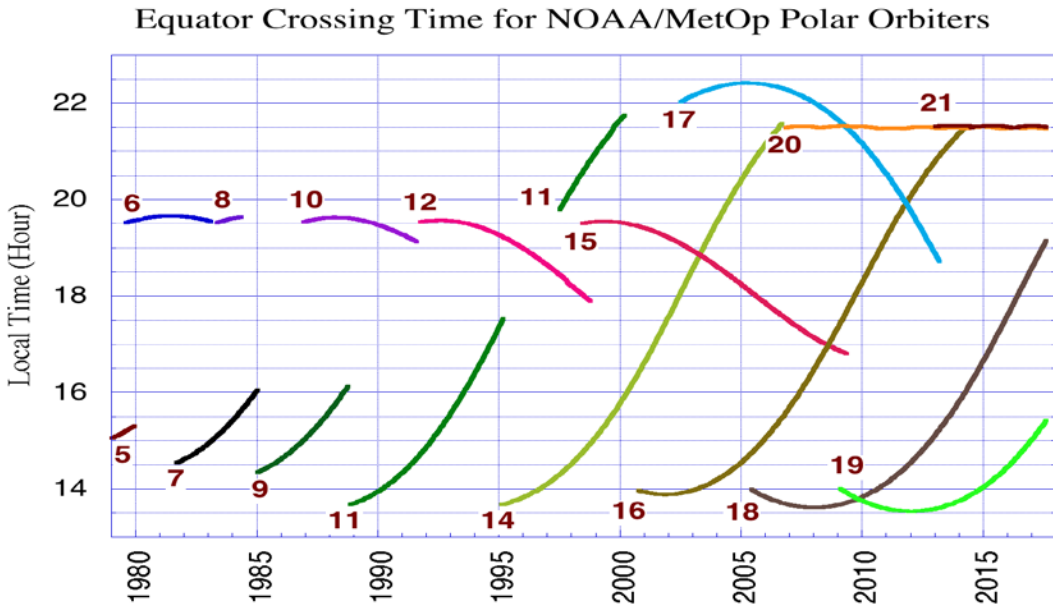


Figure 1 Equator crossing times for the ascending orbit of the NOAA POES and MetOp satellites. Refer Table 2.3 for the satellite ID labels.

3. Algorithm Description

3.1 Algorithm Overview

The multi-spectral OLR estimation method was developed by Ellingson et al. (1989) that use narrowband radiance observations from the High-resolution Infrared Sounder (HIRS) to estimate TOA total longwave flux. Vigorous validation efforts were performed for the HIRS OLR estimation technique against broadband observations derived from the Earth Radiation Budget Experiment (ERBE) and the Clouds and the Earth's Radiant Energy System (CERES) (see Ellingson et al., 1994; Lee et al., 2007). The multi-spectral OLR estimation technique has been adapted successfully to the GOES- Sounder (Ba et al., 2003) and GOES-Imager instruments (Lee et al., 2004). These studies have shown that this OLR estimation algorithm can reliably achieve with an accuracy of about 4 to 8 Wm^{-2} for various instrument type, with biases (precision) that are within the respective radiometric accuracy of the reference instruments. The HIRS OLR algorithm has been implemented to generate the NESDIS operational HIRS OLR product since September 1998, and the GOES Imager OLR is implemented as part of the operational GOES Surface and Insolation Product (GSIP). A variant of this method has been developed and implemented for the upcoming GOES-R Advanced Baseline Imager instrument (Lee et al., 2010).)

The multi-spectral OLR algorithm can be described by

$$I_{\nu}^{\uparrow}(z_i; \theta, \phi) = \varepsilon_{\nu}^* B_{\nu}^*(0) T_{\nu}^*(z_i, 0; \theta, \phi) + \int_0^{z_i} B_{\nu}(z') \frac{\partial T_{\nu}(z_i, z'; \theta, \phi)}{\partial z'} dz' \quad (3.1)$$

OLR – TOA Outgoing Longwave Radiation (Wm^{-2})

a_0 – regression coefficient, constant term (Wm^{-2})

a_i – regression coefficients, slope term, for the i^{th} predictor ($sr\ cm^{-1}$)

N_i – the i^{th} predictor of HIRS radiance ($Wm^{-2}\ (sr\ cm^{-1})^{-1}$)

θ – local zenith angle (degree)

Equation 3.1 states that the OLR can be estimated as a linear combination of a number of the selected narrowband radiances N_i , given appropriate weightings. The regression coefficients and radiances are functions of local zenith angle, θ , such that the OLR can be obtained directly from slant path observations. More explanation can be found in the Theoretical Description.

3.2 Processing Outline

The HIRS OLR CDR algorithm derives monthly mean OLR using all available HIRS radiance observations from the POES and MetOp satellites. The primary input is the HIRS Level-1b data files. This algorithm performs HIRS radiance calibration independently from

the operational calibration methods such that the radiance calibration is consistent throughout the OLR time series. Figure 2 provides the overview for the HIRS OLR CDR production system. Figure 3 is the HIRS OLR CDR production flow chart that explains the execution sequences and input/output relationships.

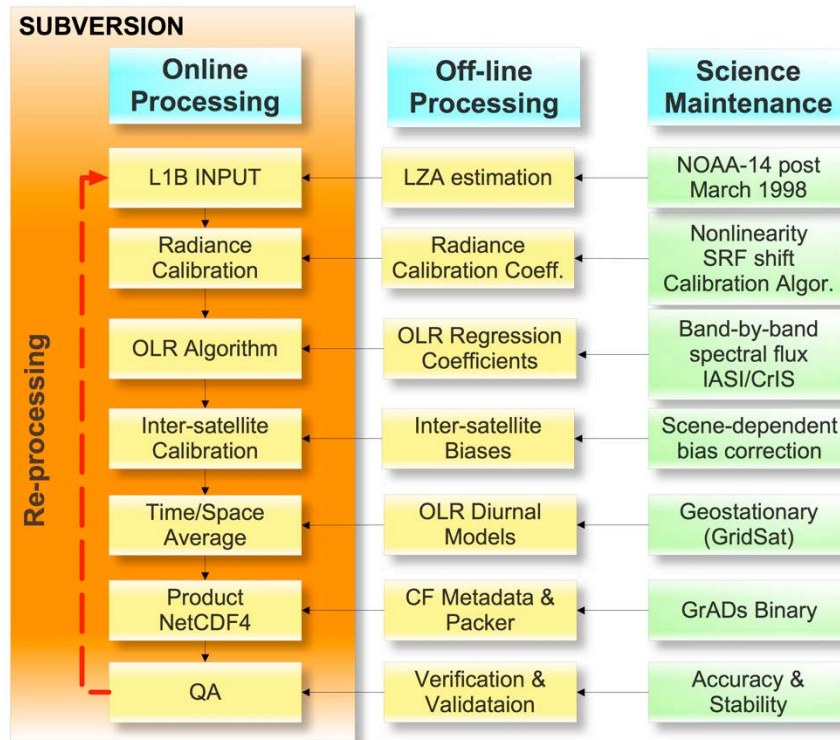


Figure 2 HIRS OLR CDR production system overview.

HIRS OLR CDR Production Flow Chart

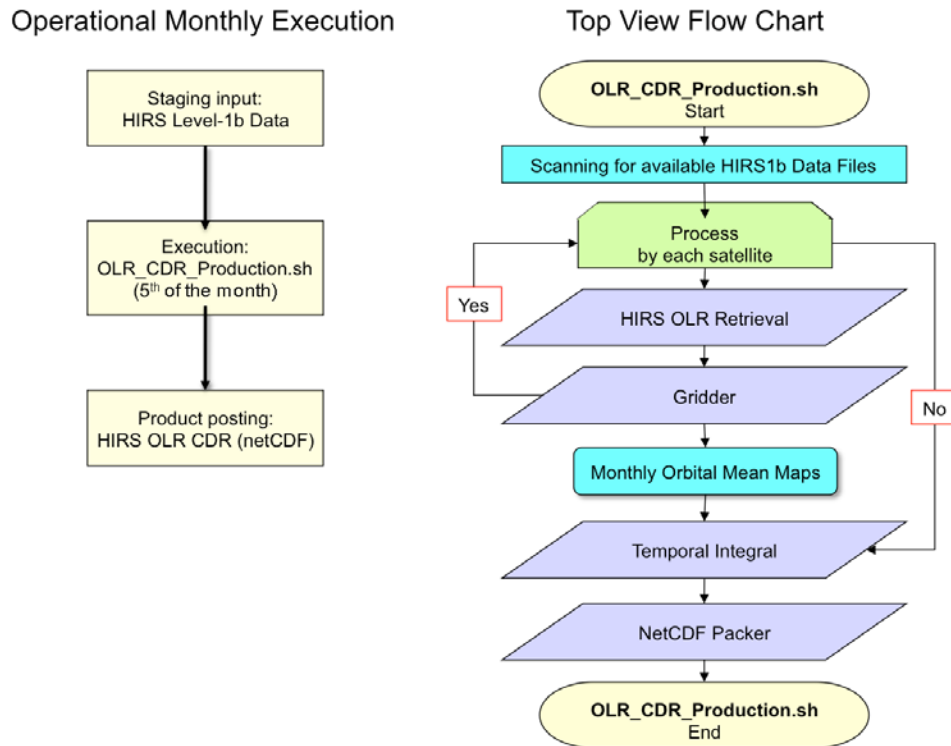


Figure 3 HIRS OLR CDR production flow chart.

3.3 Algorithm Input

3.3.1 Primary Sensor Data

The primary input data for the HIRS OLR CDR algorithm is HIRS Level-1B data from which the HIRS radiances are derived.

The HIRS OLR CDR production package includes a radiance calibration component that consistently derives HIRS radiances from the HIRS Level-1B data. The calibration module handles the variation in the format of HIRS Level-1b accordingly.

3.3.2 Ancillary Data

There are five groups of ancillary data (namely, the static data) that are required for the HIRS OLR CDR production: a) the OLR regression coefficients, b) the calibration prediction coefficients; c) OLR inter-satellite bias adjustments; d) OLR diurnal model coefficients; and e) Time stamp template. These static data in (a)-(c) are satellite-specific.

a) OLR Regression Coefficients

The coefficients for the OLR regression model are derived from a set of 3200 simulated fluxes and radiances (see Ellingson et al. 1989 and Lee et al. 2007 for details). The version of the OLR regression coefficients is defined by the version of radiative transfer model simulations. The regression coefficients included in this package were generated according to Lee et al. (2007), with a version code name "M2S2".

Format	ASCII tabulated, 5 columns x 6501 lines
Version	M2S2
Size	430K B each; Total 6.5 MB for 15 files (N05-N20).
Location	/Data_static/OLR_coef/coef_\${satid}_305_a19.asc (refer /Scripts/OLR_retrieval.sh)
Access	Local
Reference	/Documentations/Publications/Lee 2007 HIRS OLR CDR.pdf

b) Calibration Prediction Coefficients

There are sets of coefficients that are required by the McMillin radiance calibration method (NOAA POD Users Guide, 1998). They are also satellite specific. The generation and updates of these coefficients are discussed in Lee et al. (2007) and the technical report "McMillin HIRS Radiance Calibration Method".

Format	ASCII
Version	Ver.1: N05 – N12 Ver.2: N14 Ver.3: N15 – N20. (Refer /Utility/define_pred_version.sh)
Size	25 KB per satellite; Total 375 KB.
Location	/Data_static/cali_data/\${satid} (refer /Scripts/OLR_retrieval.sh)
Access	Local
Reference	/Documentations/Publications/Lee 2007 HIRS OLR CDR.pdf /Documentations/Tech_Report/McMillin HIRS Radiance Calibration Method.pdf

c) OLR Intersatellite Bias Adjustments

The methodology for deriving the bias adjustments and their recent update of these coefficients are discussed in Lee et al. (2007) and the technical report "Summary intersat calib v2.7.pdf". The Adjustment amount is to be subtracted from the OLR retrievals of the corresponding satellite.

Format ASCII
 Version Ver. 2.7
 Size 4 KB
 Location /Data_static/Intersat_Adjustment_Ed2.7.dat
 (refer /Scripts/OLR_monthly_integral.sh)
 Access Local
 Reference /Documentations/Publications/Lee 2007 HIRS OLR CDR.pdf
 /Documentations/Supplement/Intercal v2.7 determination.docx

Table 5 OLR Intersatellite Bias Adjustments, in unit Wm^{-2} .

Satellite ID	Ver.2.0 (obsolete)	Ver.2.2 (obsolete)	Ver.2.7
N05	0.15	0.00	-0.13
N06	1.80	1.62	-0.36
N07	2.13	2.18	-0.28
N08	2.03	1.84	0.00
N09	0.00	0.00	0.00
N10	0.53	0.57	-0.15
N11	-5.36	-5.04	-0.53
N12	-2.42	-2.22	-0.23
N14	-5.14	-4.63	-0.16
N15	-3.65	-3.19	0.49
N16	-3.25	-2.82	0.50
N17	NA	-3.22	0.53
N18	NA	-3.60	-0.03
N19	NA	-3.27	0.24
N20	NA	-3.56	0.10
N21	NA	TBD	-0.01

d) OLR Diurnal Model Coefficients

The construction of the climatological OLR diurnal models is discussed in details in Lee et al. (2007). These models described the climatological OLR diurnal variations for each month at each of the $2.5^{\circ} \times 2.5^{\circ}$ region on the monthly mean basis. They are used in the OLR monthly mean temporal integral calculations.

Format IEEE Binary
 (direct access, unformatted, record length= $4 \times 144 \times 72 \times 12 \times 4$ Bytes)

A controlled copy of this document is maintained in the CDR Program Library.
 Approved for public release. Distribution is unlimited.

(refer /Codes/Temporal/OLR_monthly_integral.f90)

Version Ver.1

Size 2 MB

Location /Data_static/coef_diurnal_model.dat
(refer /Scripts/OLR_monthly_integral.sh)

Access Local

Reference /Documentations/Publications/Lee 2007 HIRS OLR CDR.pdf

e) Time Stamp Template

The time stamp template file contains time markers as the increments in days (real number) since Jan 1. 1979 00:00:00Z. These predefined time markers include the time at the exact middle, and the beginning and the ending bounds for each month.

Format ASCII
(refer /Codes/Packer/OLR_CDR_nc4_batch.f90)

Version Ver.1

Size 12 KB

Location /Data_static/Time_template_720.dat
(refer /Scripts/packer_batch.sh)

Access Local

Reference /Documentations/Publications/Lee 2007 HIRS OLR CDR.pdf

3.3.3 Derived Data

Not applicable.

Remark: The radiance calibration module takes the HIRS Level-1B data as the input and derives the HIRS radiance. The radiance is then passed directly to the OLR regression model without being written to an intermediate data file.

3.3.4 Forward Models

Not applicable.

3.4 Theoretical Description

The HIRS CDR OLR production is a sequential processing. The sequence and the relevant processing are described here. See "OLR_CDR_Production.sh" script file for more details.

(1) Radiance Calibration

The HIRS OLR CDR production starts with the derivation of the radiance from the HIRS Level-1B data by the radiance calibration module. The radiance calibration is performed

consistently throughout the HIRS OLR time series with the McMillin radiance calibration method.

(2) OLR Retrieval

The multi-spectral OLR estimation technique is applied here. The OLR is retrieved at each HIRS FOV with the given radiances and local zenith angles.

(3) Gridding of OLR Monthly Orbital Maps

For each satellite, one month worth of FOV OLR retrievals are compiled and gridded into two 2.5°x2.5° equal-angle maps, consisting of observations from the ascending and descending orbits, respectively. The attribution of the ascending/descending orbit is determined as the 12-hour interval centered on the corresponding equator crossing times, which are determined from the HIRS1b data directly.

(4) Temporal Integration for Monthly Mean and Intersatellite Bias Adjustment

The OLR monthly mean is derived from the gridded OLR monthly orbital maps of all the contributing satellites. The monthly orbital maps can be considered as the monthly mean OLR at particular local times.

The OLR intersatellite bias adjustments are first applied to the OLR monthly orbital maps before the temporal integration. Then the temporal integral is independently performed for each of the 144x72 grids.

The diurnal variation envelop prescribed by the OLR diurnal models is constrained by the observed OLR retrievals obtained at different observing local times. The OLR monthly mean value is then determined as the integral of the constrained envelop curve over the 24 hours period.

(5) NetCDF packing

The last step is NetCDF packing for the release product file. The HIRS OLR CDR product is a single NetCDF file that contains the entire time series starting on January 1979. The newly retrieved monthly mean OLR data will be added to the existing time series and a new NetCDF product file will be generated for release.

3.4.1 Physical and Mathematical Description

The specific intensity I_ν of upward longwave radiation at the top of the atmosphere z_t at local zenith angle θ and azimuth angle ϕ . can be expressed as:

$$I_\nu^\uparrow(z_t; \theta, \phi) = \varepsilon_\nu^* B_\nu^*(0) T_\nu^*(z_t, 0; \theta, \phi) + \int_0^{z_t} B_\nu(z') \frac{\partial T_\nu(z_t, z'; \theta, \phi)}{\partial z'} dz' \quad (3.2)$$

where T_ν is the monochromatic atmospheric transmittance, T_ν denotes the surface emissivity, $B_\nu(z')$ is the Planck function evaluated at wave number ν with the temperature at level z' . The black surface is assumed here.

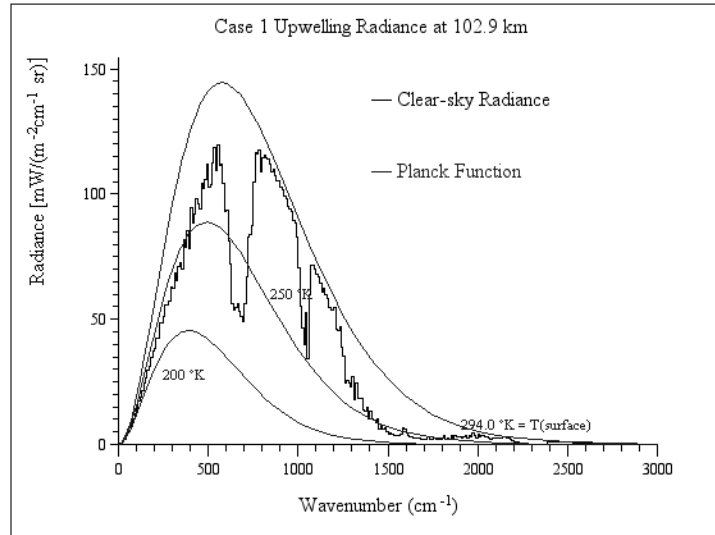


Figure 4 TOA upward longwave radiation spectrum for standard mid-latitude summer case. The smooth curves are the Planck function evaluated at 200°K, 250°K and 294°K (surface temperature for this case), respectively for reference purpose.

The outgoing longwave radiation (*OLR*), whose example spectrum is shown in Figure 4, is the radiative flux through a unit area at the top of the atmosphere that is related to the specific intensity by integrating over wavenumbers (ν) and over hemispheric solid angles (θ and ϕ):

$$OLR = \int_0^{2\pi} \int_0^{\pi/2} \int_0^{\infty} I_{\nu}^{\uparrow}(z_i; \theta, \phi) \cos \theta d\nu \sin \theta d\theta d\phi \quad (3.3)$$

Ellingson et al. (1989) formulated the multi-spectral OLR algorithm that expresses the OLR as a linear combination of the radiances (N_i) of selected channels, observed at a local zenith angle θ :

$$OLR = a_0(\theta) + \sum_i a_i(\theta) \cdot N_i(\theta) \quad (3.4)$$

The satellite-observed narrowband radiance N_i of channel i can be described by the convolution of the TOA specific intensity with the respected spectral response function Φ_i

$$N_i(\theta, \phi) = \int_{\Omega_{\nu_i}} I_{\nu}^{\uparrow}(z_i; \theta, \phi) \cdot \Phi_i(\nu) d\nu \quad (3.5)$$

The azimuth angle dependence in the radiance is removed when axel-symmetry is assumed.

The bounds of the wavenumber integral for OLR are 0 to 3000 cm^{-1} .

3.4.2 Data Merging Strategy

The HIRS OLR CDR production uses multi-platforms observations that require critical data merging techniques to achieve consistency and continuity. Special cares are needed in OLR retrieval and temporal integration aspects.

OLR retrieval

Obtaining consistent OLR retrievals from all satellites is achieved through two controlling factors: 1) consistent OLR regression models; 2) inter-satellite calibration.

The coefficients for OLR regression models are satellite/instrument specific. Since the coefficients are derived from a common set of simulations, the OLR regression models for different satellites and instruments would have consistent error characteristics, if the instruments are not changed. However, due to the variations in HIRS/2/2I/3, and 4, there are necessary changes in the OLR regression model formulation, which could result in inconsistencies in their regression error characteristics. This in turn will reduce the robustness of the inter-satellite calibration results.

There are other factors that can affect the accuracy of the OLR retrievals but not yet fully resolvable at the moment, e.g., consideration of sensor non-linear response and uncertainties in spectral response functions. The current approach is to remove the bulk intersatellite OLR biases by directly comparing OLR retrievals between two satellites with collocated observations. This is a first order end-to-end correction on all the possible errors for the OLR retrievals from radiance calibration to the OLR model application.

Temporal Integral

Polar orbiters have low temporal sampling rate – twice a day for a given location from each satellite. Although composite observations can be obtained from multiple polar orbiters, the orbital drift effects can alias into artifacts or spurious trends for the time series if temporal integral is not performed carefully. As an approximation, the HIRS OLR CDR uses the climatological OLR diurnal models to reduce the temporal integral errors related to orbital drifts. A better accuracy can be obtained when using OLR estimated from geostationary satellites. And this is for future improvement.

3.4.3 Numerical Strategy

Missing Value and Weaver Subroutine

The monthly mean OLR map could have missing values if the temporal integral performed at certain grid boxes failed, possibly due to insufficient OLR retrieval data. (Note that this is extremely rare if there are two or more satellites in a given month.) Approximations for such grids will be made with the Cressman interpolation (Cressman, 1959) by the Weaver subroutine.

3.4.4 Calculations

The HIRS OLR CDR Production includes the following steps:

- a) Compile.sh – clean compilation of all Fortran programs
- b) OLR_CDR_Production.sh - HIRS OLR CDR Production driver script
- c) OLR_retrieval.sh – HIRS radiance calibration and OLR retrieval
- d) OLR_gridder.sh – Gridding of orbital map
- e) OLR_monthly_integral.sh – Intersatellite bias adjustment and monthly mean temporal integral
- f) OLR_packer_batch.sh – Pack into NetCDF-4 product file

a) Compile.sh

- Compilation of all Fortran programs used in OLR CDR Production.

b) OLR_CDR_Production.sh

- Main driving script for HIRS OLR CDR production.
- In automated mode, it is to be executed once a month, presumed to be on the 5th day of a month.
- It can also be invoked with an argument of <yyyymm> to specify the month to be processed.

c) OLR_retrieval.sh

- Perform HIRS radiance calibration
- Retrieve OLR at each HIRS field of view (FOV)

d) OLR_gridder.sh

- Create OLR orbital maps for ascending and descending node respectively at 2.5°x2.5° equal-angle grid.

e) OLR_monthly_integral.sh

- Giving the monthly orbital mean maps from the available satellites, perform monthly mean integral constrained with OLR diurnal models.
- Integral is constrained with the climatological OLR diurnal models (monthly, 2.5°x2.5° in ECT time stamp).

f) OLR_packer_batch.sh

- Pack OLR CDR data into a NetCDF4 data file, including the previously derived months and the newly derived OLR monthly mean data stored in Work/OLR_CDR/archive_ascii/.

3.4.5 Look-Up Table Description

Radiance Calibration: Band parameters

Origin NOAA POD and KLM Users Guide
Construction 4 x 19 per satellite, in ASCII
Usage Define HIRS channel band central wavenumber and correction coefficients

Radiance Calibration: PRT Coefficients

Origin NOAA POD and KLM Users Guide
Construction 6 x 4 per satellite (N05-N14), in ASCII
5 x 5 per satellite (N15-N17), in ASCII
7 x 5 per satellite (N15-N20), in ASCII
Usage Define HIRS PRT count to temperature conversion coefficients

Radiance Calibration: Temperature prediction coefficients

Origin Hai-Tien Lee. CICS/UMD
Construction 9 x 19 x 2, in ASCII
Usage Define temperature prediction coefficients to estimate temperature-dependent calibration coefficients

OLR Regression Coefficients

Origin Hai-Tien Lee. CICS/UMD
Construction 8 x 6500 in ASCII
Usage Construct OLR regression models

Inter-satellite Bias Adjustment

Origin Hai-Tien Lee. CICS/UMD
Construction 16 x 1 in ASCII
Usage Define OLR bias adjustments (Wm^{-2})

Coefficients for OLR Diurnal Models

Origin Hai-Tien Lee. CICS/UMD
 Construction 3 x 144 x 72 Binary
 Usage Define OLR diurnal models

Time markers for HIRS OLR CDR time series

Origin Hai-Tien Lee. CICS/UMD
 Construction 7 x 720 ASCII
 Usage Define time markers for the monthly mean: center, lower and upper bounds

3.4.6 Parameterization

None.

3.4.7 Algorithm Output

Name HIRS Monthly Mean OLR Time Series
 Content Global 2.5°x2.5° gridded monthly mean OLR time series from 1979 to the presently processed month
 File Format NetCDF4
 Specific Data hirs_olr_mon_v02r07_197901_201612.nc
 (note that the ending time "201612" will be changed accordingly)
 Physical Unit Wm⁻²
 Size 19 MB (for 38 years of monthly mean data)

4. Test Datasets and Outputs

4.1 Test Input Datasets

The test input datasets consist the entire HIRS level1b data available as of Sept. 1, 2017.

4.2 Test Output Analysis

4.2.1 Reproducibility

To test the reproducibility of the Rejuvenated OLR CDR package against the baseline version of the v02r07 processing system at CICS, the differences of the monthly mean values were examined. The Rejuvenated OLR CDR package is the one to be used for official production of v02r07, while evaluations/validations were conducted with the output from the baseline version. Therefore we need to examine the reproducibility for the code packages

Figures. 5 and 6 summarize the statistics of the comparison by showing the average and standard deviation of the global monthly mean OLR differences between the rejuvenated and the baseline v02r07 processing packages. Most of the differences are related to the increased number of retrievals in the rejuvenated version, which improves the ability to construct of the “super data”. (The super data is a processing unit that contains HIRS earth-view scan lines encompassed by the warm/cold calibration scans at both ends.) In the baseline version, many superdata were abandoned when there are some missing scans.

The range of the average and standard deviation of the global monthly OLR differences are within expectation that we consider the reproducibility is maintained.

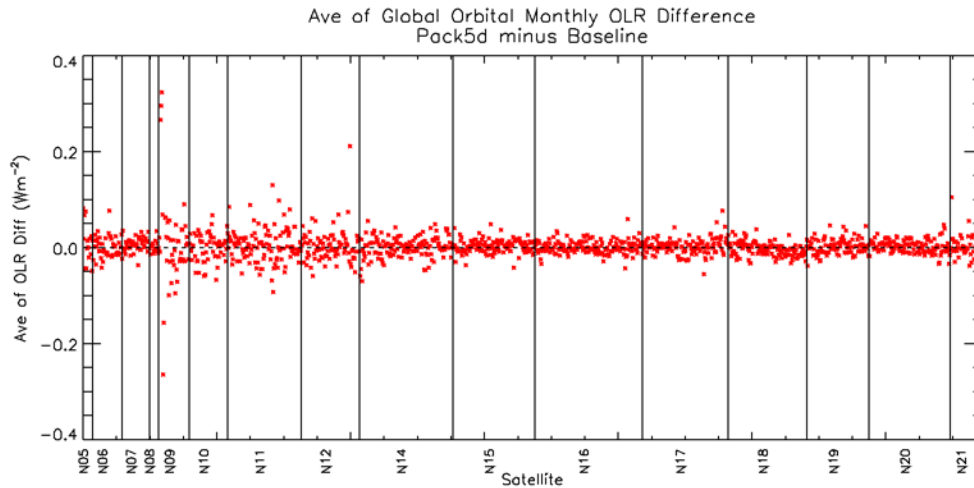


Figure 5 Differences of Global mean OLR CDR between the Rejuvenated and the baseline version of the v02r07 code packages. (Rejuvenated version is labeled as “Pack5d”)

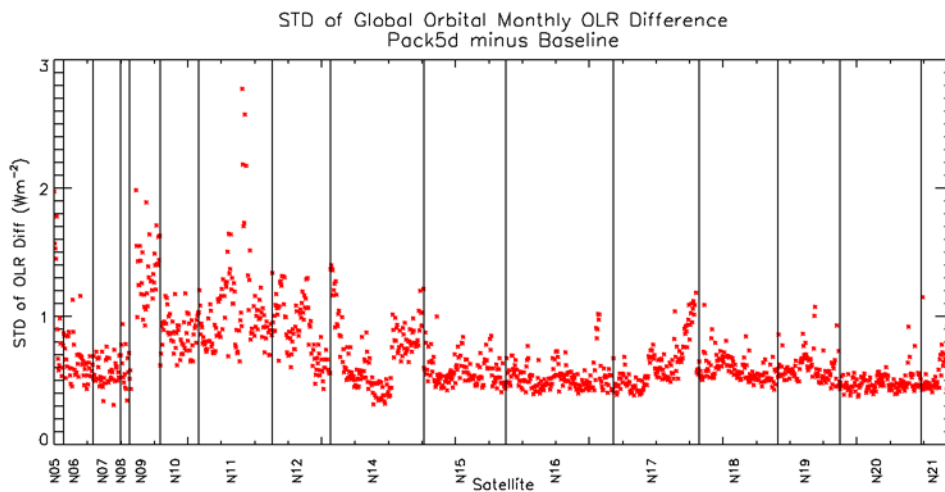


Figure 6 Similar to Figure 5 but is for the standard deviation of the global monthly mean OLR differences.

4.2.2 Precision and Accuracy

The precision and accuracy of the HIRS OLR CDR product are determined by the comparisons to the reference broadband OLR products, currently the CERES EBAF Ed4.0 OLR product.

The current assessment of the HIRS OLR CDR is to have a precision within 2 Wm^{-2} (with an about -2 Wm^{-2} overall bias) and an accuracy of about 2.5 Wm^{-2} , relative to the CERES EBAF Ed.4.0 OLR product

Figures 7-13 show the various comparison results for the accuracy assessments.

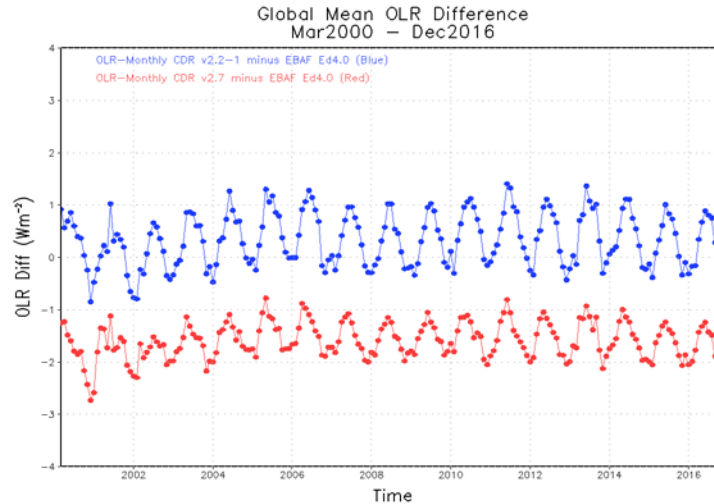


Figure 7 Time series of the global mean monthly OLR, OLR CDR minus EBAF. (Blue: OLR CDR v02r02-1; Red: v02r07) The smaller disagreement in the annual cycle discrepancies is an evidence of the improvements in v02r07. Note that the EBAF Ed.4 OLR has been adjusted upwards by an about 0.5 Wm^{-2} relative to Ed2.8. The trended differences between 2000-2003 are related to the relatively larger uncertainties in the EBAF data that was constructed with TERRA CERES observations only.

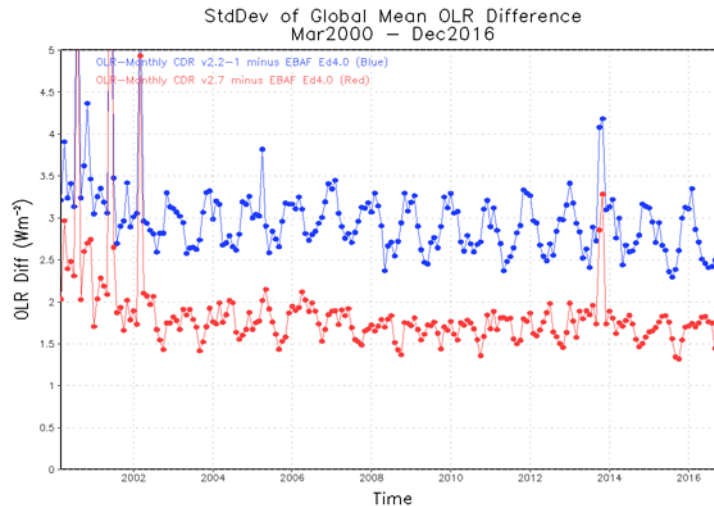


Figure 8 Similar to Figure 7 but for the standard deviation. The OLR CDR v02r07 has improved significantly in both the annual cycle amplitude as well the spatial distribution, relative to the EBAF Ed4 data. The standard deviation of the regional differences in the two products is below 2 Wm^{-2} . The spikes shown in the earlier period and one near 2014 are due to the sampling differences, mostly due to the missing data in MODIS that prevents CERES from generating products.

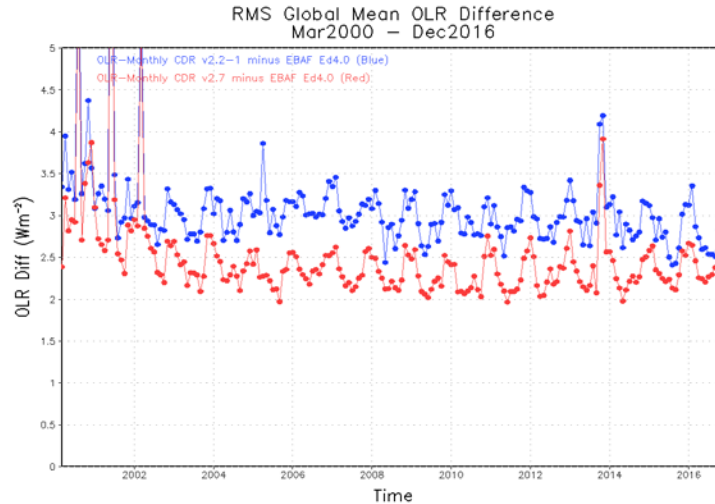


Figure 9 Similar to Figure 7 but for the RMS differences. The OLR CDR v02r07 has improved the overall agreement of the spatial distribution, relative to the EBAF Ed4 data. The RMS of the regional differences in the two products is at about 2.5 Wm^{-2} level.

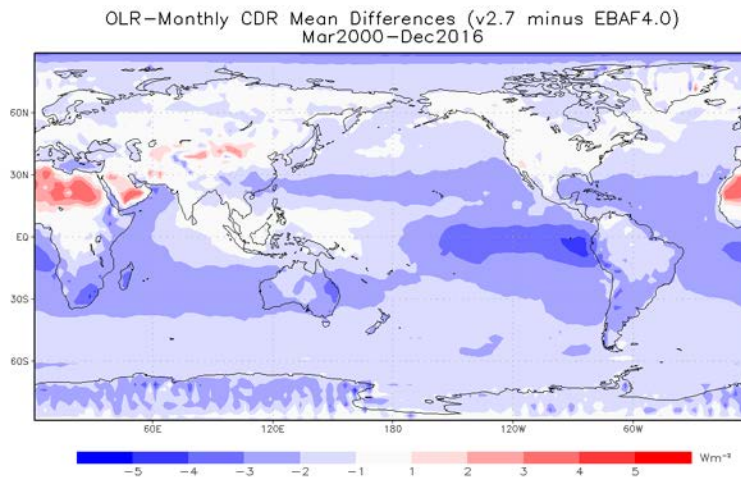


Figure 10 Averaged regional OLR differences between OLR CDR v02r07 and EBAF Ed4, over the period of March 2000 to Dec 2016. Two profound geographical features can be identified: a) desert areas over the North Africa; b) sub-tropical, especially near the eastern Pacific Ocean. These are the problems for future improvements.

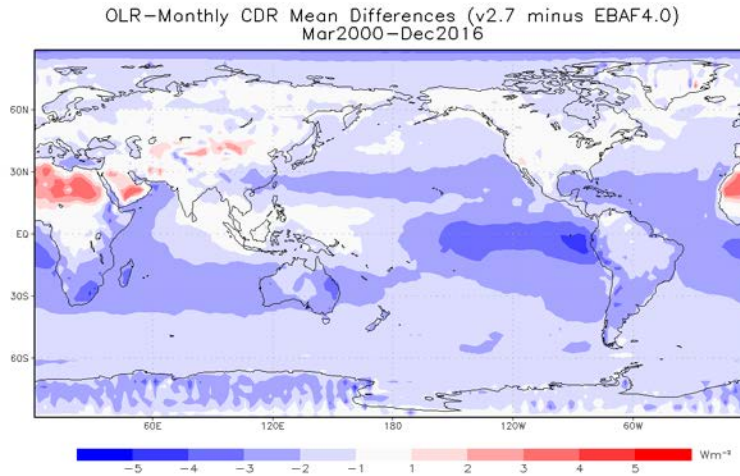


Figure 11 Averaged regional OLR differences between OLR CDR v02r07 and EBAF Ed4, over the period of March 2000 to Dec 2016. Two profound geographical features can be identified: a) desert areas over the North Africa; b) sub-tropical, especially near the eastern Pacific Ocean. These are the problems for future improvements.

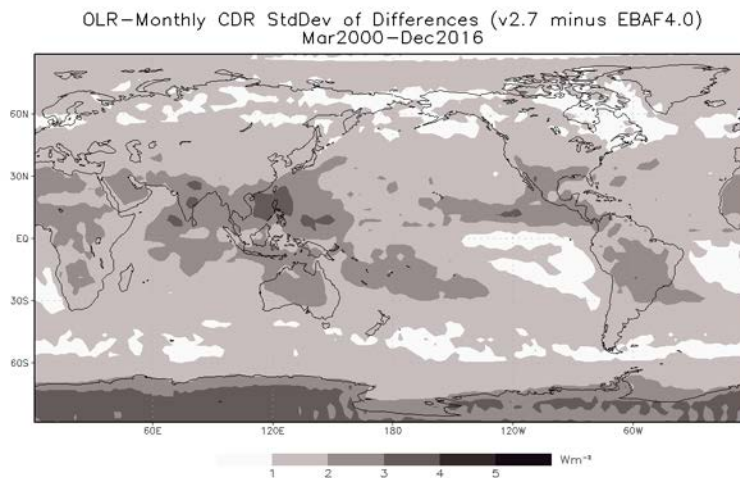


Figure 12 Similar to Figure 11 but is for the Standard deviation of the OLR differences. The largest random errors were found in the western Pacific warm pool and over the Antarctica.

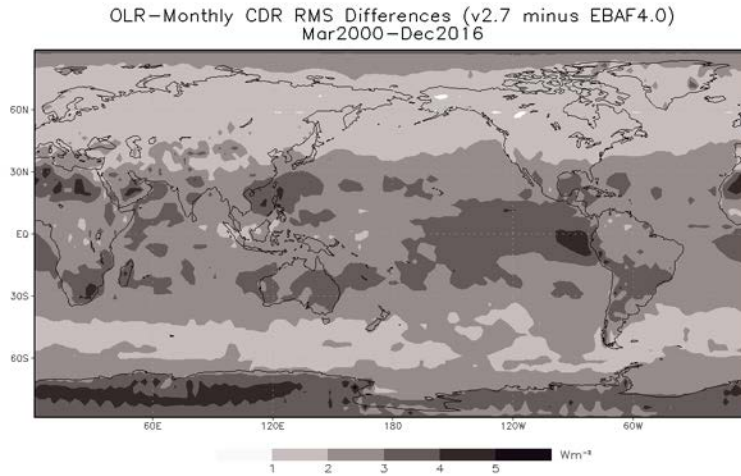


Figure 13 Similar to Figure 11 but is for the RMS differences. The relatively larger discrepancies were found over the eastern tropical Pacific Ocean, Sahara deserts, and the eastern Antarctica.

4.2.3 Error Budget

The possible sources of error for HIRS OLR CDR derivation are listed in Table 4.3. The best estimates of their magnitude of errors are given. Note that those errors cannot be aggregated in a simple form.

Table 6 Error sources and best estimated magnitude for HIRS OLR CDR production.

Error Sources	Magnitude of Errors	Prospective Improvements
Radiance Calibration	bias at ~0.5°K	<ul style="list-style-type: none"> ○ non-linear calibration method; ○ estimate of post-launch spectral response function;
OLR retrieval	RMS errors ~2 to 3 Wm ⁻²	<ul style="list-style-type: none"> ○ More accurate OLR estimation model, e.g., band-by-band
Intersatellite calibration	biases at ~1 to 2 Wm ⁻²	<ul style="list-style-type: none"> ○ Scene dependent bias adjustments; ○ More consistent OLR models across HIRS instrument versions;
Navigation (Local Zenith Angle error in N14)	~30°	<ul style="list-style-type: none"> ○ Redo HIRS1b navigation ○ Assume constant satellite view angles ○ construct empirical estimation of LZA
Temporal integral	?	<ul style="list-style-type: none"> ○ Use of geostationary observations to better describe the OLR diurnal variation

5. Practical Considerations

5.1 Numerical Computation Considerations

Endian

The HIRS OLR CDR Production Package assumes IEEE big-endian environment.

Precision

The codes can be run under either 32-bit or 64-bit mode.

Parallelization

This production package is considered not computationally intensive that explicit parallelization is not performed.

5.2 Programming and Procedural Considerations

None.

5.3 Quality Assessment and Diagnostics

Quality flags and automatic diagnostics will be implemented.

5.4 Exception Handling

Gridder.f90

The equator crossing time cannot be determined when there are insufficient numbers of near equator observations in a given orbit file. The ECT will be considered missing and is assigned to -1 when that is the case returning to calling routine. The monthly mean ECT determination (in grid_OLR.f90) will skip those missing ECT during averaging.

OLR_monthly_integral.sh

In initial design that this script will exit when the number of OLR FOV retrieval output files for a given satellite is less than 15. Currently this threshold is defined at 0, effectively removing this criteria. Be cautious when HIRS-1b data is only partially available in a given month.

OLR_monthly_integral.f90

This program will stop when the read statement for reading the coefficients of the OLR diurnal models encounters error. Currently there is no error handling of such incident. The monthly mean OLR ASCII output file will not be generated when this happens. (And the netCDF packaging will not generate any result either.). Human interruption is required in this case to resolve the directory/file location error.

OLR CDR nc4 batch.f90

The packing of NetCDF parameters is subject to error check, by subroutine `check_err`. The program will exit if any errors were detected. This will cause failure in the generation of NetCDF product file. This condition will be written to the process log and human interruption will be required.

5.5 Algorithm Validation

Summary

The production and validation of the HIRS OLR CDR Ver.02 Rev.00 (time series 1979-2003) is described in Lee et al. (2007). This validation has shown that the HIRS OLR CDR time series has stability comparable to that of the Earth Radiation Budget Satellite (ERBS) non-scanner OLR measurements, at about 0.3 Wm^{-2} per decade. Globally, HIRS OLR agrees with CERES with an accuracy to within 2 Wm^{-2} and a precision of about 4 Wm^{-2} .

The assessments for the revised OLR CDR v02r07 against the updated CERES OLR EBAF Ed4.0 product show significant improvements over those previously established. The over accuracy is now assessed to be at about 2.5 Wm^{-2} . The most important improvement is in the removal of the spurious trend present in the v02r02 product.

Validation Strategy

The HIRS OLR retrieval and its monthly mean product are evaluated with the radiative flux measurements from broadband instruments, including the ERBS non-scanner, ERBE scanners, and CERES scanners.

For the instantaneous retrieval accuracy assessment, HIRS OLR retrieval at HIRS FOV is compared against the ERBE/CERES Level-2 single scanner footprint (SSF) product, where the broadband radiance measurement is converted to the total flux at FOV level.

For the monthly mean product evaluation, currently the best validation reference is the CERES Level-3 Monthly TOA/Surface Average (SRBAVG) product that derives the monthly mean with the assistance of the geostationary satellite observations. The HIRS OLR CDR Ver.2.0 was validated against ERBE S-4 monthly mean data sets and CERES ES-4 monthly mean data sets. Validation of HIRS OLR CDR with more recent releases of CERES products is ongoing.

There are upcoming improvements in the broadband OLR products as well, include the CERES Ed3 release that would have better estimate and handling of the sensor degradation. And the ERBE scanner OLR will be re-derived with revised angular distribution model (ADM) and possibly better temporal integration. Repeating the systematic validations for HIRS OLR CDR with the latest release of the broadband products is highly recommended.

The inter-comparison of the HIRS OLR CDR product with other OLR products and model simulations is a continuing effort. Multiple sets of inter-comparisons enable us to

identify problems in the data sets that are otherwise difficult to affirm. These exercises can raise the confidence level of the validation assessments.

5.6 Processing Environment and Resources

Computer Hardware: Mac Pro 2x2.4GHz Quad-Core Intel Xeon, 20GB memory

Operating System: Mac OS X 10.6.8

Programming Language: Fortran90

Compilers: Intel Fortran v11.1

External Libraries: NetCDF 4.1.1

CPU Time: 570.346 seconds

Wall Clock Time: about 21 minutes

Temporary Storage: 2.5 GB/month (~0.5GB per satellite per month of OLR_fov outputs)

6. Assumptions and Limitations

Radiative Transfer Model Simulations

The OLR regression models were constructed with a set of radiative transfer model simulations. As being statistical models, they are assumed to be representative for global application in all sky conditions. Scene-dependent errors might be traceable to this assumption and modeling improvements would be necessary to eliminate such errors.

Intersatellite Calibration

The inter-satellite bias adjustments are determined with the collocated observations during the overlapping period for two satellites. Since the majority of collocations occur in the Polar Regions that the derived biases may not be representative for other climate zones. This requires confirmation and improvements when necessary.

OLR Diurnal Model

The accuracy of monthly mean temporal integration is limited by the temporal sampling rate and integration method employed. The current HIRS OLR CDR production uses climatological OLR diurnal models to estimate monthly mean. It assumes, on the monthly mean basis, that the magnitude of inter-annual/decadal variation in OLR diurnal cycle is much smaller than that of the OLR diurnal cycle itself. This is quite valid over land but may not always hold true over the ocean, e.g., the large change in cloudiness in equatorial Pacific during El Niño years.

The use of OLR diurnal models indeed helps to reduce artifacts caused by the orbital drift and changes of observation time, but more accurate temporal integration could be attained with OLR observed/estimated from geostationary satellites.

Navigation

The HIRS OLR CDR production uses HIRS level-1b data as the primary input. It assumes that the navigation parameters, including the coordinates and viewing geometry for the earth FOV locations, are correct. There are known errors: incorrect local zenith angle data in NOAA14 post March 1999 would degrade the OLR retrieval quality. Such errors need to be dealt with offline.

6.1 Algorithm Performance

The OLR retrieval will be performed when the radiances from the required HIRS channels are available, otherwise, the OLR retrieval will not be performed. There are possible degradation paths for the OLR retrievals using different sets of prediction channels. However, these degradation paths are yet to be explored and currently undefined.

6.2 Sensor Performance

Radiometric Calibration

The HIRS OLR CDR production performs radiance calibration following McMillin method. A set of coefficients is used in predicting calibration coefficients. This is to introduce instrument temperature dependence for the interpolation of the calibration coefficients between two calibration cycles. These coefficients may require updates when the instrument temperatures have shifted significantly from the existing samples.

Radiometric Noise

The HIRS OLR CDR production package examines the quality flags of the HIRS level-1b data to determine if OLR retrieval can be performed. The OLR retrieval will still be performed when the sensor radiometric noise is higher than the instrument specification but the quality flag is not turned on. There are several problems in the recent HIRS instruments since NOAA-15 that requires ad hoc examination to determine a better quality control for OLR retrieval purpose.

Spectral Response Function

The spectral response function has a role in the radiance calibration and in the radiance simulation. The accuracy of OLR estimation depends on the radiative transfer model simulations of the OLR flux and the HIRS radiances. Errors will be introduced if the pre-launch response function characterization is incorrect or the response functions have changed post-launch.

Instrument Scanning Alignment

There are known errors in the HIRS scanning operation on NOAA15 and 16. It is currently believed that the scanning is off by one scanning step position, in both satellites. Correction in the navigation parameters has already been applied in the level-1b data. Users should be aware of this error and use these data more cautiously.

7. Future Enhancements

7.1 Enhancement 1 - OLR Model for IASI and CrIS

The last pair of morning/afternoon HIRS instruments on NOAA19 and MetOp-2 has been passing or nearing their design life span, 5 years. It is in urgent need that we develop the OLR retrieval algorithm for IASI and CrIS instrument to maintain the continuity of the OLR CDR data product. Preliminary IASI OLR algorithm has shown to be very accurate (Turner et al, 2015).

It is critically important that the IASI/CrIS OLR retrievals are consistent with those from HIRS.

7.2 Enhancement 2 - OLR Regression Model

The regression error of the OLR model is the largest contributor towards the HIRS OLR CDR product's error budget. Although the magnitude of the regression error might only be reduced by a limited amount given similar degrees of information content, the error characteristics can be improved significantly when a better regression form is used. Band-by-band modeling approach is very promising to eliminate scene-dependent biases by independently estimating the variations in the water vapor absorptions and surface/cloud emission. Investigations of the desert overestimation and the subtropical underestimation are also needed.

7.3 Enhancement 3 - Intersatellite Calibration

The intersatellite bias adjustments are typically derived using collocation data found in the Polar Regions. The narrow range of the OLR variability limits the investigation for scene dependence of intersatellite biases. There are four sets of near-overlapping orbital configuration in the recent years that could provide a rare opportunity to better understand this question and develop more robust inter-satellite bias corrections. The improvements over the consistency in OLR models will also lead to higher degrees of confidence in the intersatellite bias adjustments.

7.4 Enhancement 4 - Radiance Calibration

The current radiance calibration algorithm does not consider the nonlinearity of the sensor, leading to errors in the magnitude of about 0.5°K biases for cold scenes. Larger biases can also occur for hot scenes (>> 285°K). The accuracy in the pre-launch spectral response function characterization is another concern. Recent researches comparing HIRS and IASI suggest that certain amount of band shifts could provide more agreeable radiance observations (Cao, 2011, personal communication), pointing to the possibilities of inaccurate pre-launch characterization and/or post-launch instrument change.

7.5 Enhancement 5 - Limb darkening error

Comparisons of the collocated angle-matched OLR retrievals between the HIRS algorithm and the CERES SSF products showed the dependency in viewing angles. This is related to the differences of the limb darkening properties between the theoretical estimated with the one that CERES empirically constructed. As the GERB OLR product also presents similar error properties, we will investigate both the possible underestimate of the limb darkening of theoretical model, as well the error amplification from the possible CERES SW unfiltering errors.

8. References

- Ba, M., R. G. Ellingson and A. Gruber, 2003: Validation of a technique for estimating OLR with the GOES sounder. *J. Atmos. Ocean. Tech.*, **20**, 79-89.
- Cressman, G. P., 1959: An operational objective analysis system. *Mon. Wea. Rev.*, **87**, 367-374. Ellingson, R. G. and M. Ba, 2003: A study of diurnal variation of OLR from the GOES Sounder. *J. Atmos. Ocean. Tech.*, **20**, 90-98.
- Ellingson, R. G. and J. C. Gille, 1978: An infrared radiative transfer model. Part 1: Model description and comparison of observations with calculations. *J. Atmos. Sci.*, **35**, 523-545.
- Ellingson, R. G., H.-T. Lee, D. Yanuk and A. Gruber, 1994: Validation of a technique for estimating outgoing longwave radiation from HIRS radiance observations, *J. Atmos. Ocean. Tech.*, **11**, 357-365.
- Ellingson, R. G., D. J. Yanuk, H.-T. Lee and A. Gruber, 1989: A technique for estimating outgoing longwave radiation from HIRS radiance observations. *J. Atmos. Ocean. Tech.*, **6**, 706-711.
- Harries, J.E., J.E. Russell, J.A. Hanafin, et al., 2005: The geostationary Earth Radiation Budget Project. *Bull. Amer. Meteor. Soc.*, **86**, 945-960.
- Gruber, A., R. G. Ellingson, P. Ardanuy, M. Weiss, S.-K. Yang and S. N. Oh, 1994: A comparison of ERBE and AVHRR longwave flux estimates. *Bull. Amer. Meteor. Soc.*, **75**, 2115-2130.
- Gruber, A., and T. S. Chen, 1988: Diurnal variation of outgoing longwave radiation. *J. Climatol.*, **8**, 1-16.
- Gruber, A., H.-T. Lee and R. G. Ellingson, 2004: Climate monitoring with HIRS outgoing longwave radiation data. The 13th Conference on Satellite Meteorology and Oceanography. September 20-23, 2004, Norfolk, VA.
- Jackson, D. L., J. J. Bates and D. P. Wylie, 2003: The HIRS Pathfinder radiance data set (1979-2001). Proceedings of 12th Conference on Satellite Meteorology and Oceanography, Long Beach, California, February 10-13, 2003.
- Jacobowitz, H., L. L. Stowe, G. Ohring, A. Heidinger, K. Knapp and N. R. Nalli, 2003: The Advanced Very High Resolution Radiometer Pathfinder Atmosphere (PATMOS) climate dataset: a resource for climate research. *Bull. of Amer. Meteor. Soc.*, **84**, 785-793.
- Lee, H.-T., A. Heidinger, A. Gruber and R. G. Ellingson, 2004a: The HIRS Outgoing Longwave Radiation product from hybrid polar and geosynchronous satellite observations. *Advances in Space Research*, **33**, 1120-1124.
- Lee, H.-T., A. Gruber and R. G. Ellingson, 2004b: Inter-satellite calibration of HIRS outgoing longwave radiation data. The 13th Conference on Satellite Meteorology and Oceanography. September 20-23, 2004, Norfolk, VA.
- Lee, H.-T., I. Laszlo, and A. Gruber, 2010a: ABI Earth Radiation Budget - Outgoing Longwave Radiation. NOAA NESDIS Center for Satellite Applications and Research (STAR) Algorithm Theoretical Basis Document (ATBD)
- Lee, H.-T., A. Gruber and J. Lee, 2010b: Operational Generation of the HIRS Outgoing Longwave Radiation Climate Data Record. Scientific Data Stewardship Annual Meeting. Sept 14-15, 2010. NCDC, Asheville, NC

- Lee, H.-T., 2011: Sustainability of HIRS OLR Climate Data Record From Research to Operation. First Conference on Transition of Research to Operations: Successes, Plans and Challenges. 91st AMS Annual Meeting, Seattle, WA, January 23-27, 2011.
- Lee, H.-T. and R. G. Ellingson, 2013: HIRS OLR Climate Data Record - Production and Validation Updates. Proceedings of the 2012 International Radiation Symposium (IRS'2012). AIP Conf. Proc., 1531, 420 (2013); doi: 10.1063/1.4804796
- Lee, H.-T., 2014: Daily OLR Climate Data Record – A challenge to homogenize operational satellite observations for climate applications. EGU General Assembly 2014.
- GCOS: <http://www.wmo.int/pages/prog/gcos/index.php?name=EssentialClimateVariables> (as of July 19, 2011)
- NOAA Polar Orbiter Data (POD) User's Guide: 1998 version available online at <http://www.ncdc.noaa.gov/oa/pod-guide/ncdc/docs/intro.htm> as of July 18, 2011.
- NOAA KLM User's Guide: Feb. 2009 version available online at <http://www.ncdc.noaa.gov/oa/pod-guide/ncdc/docs/intro.htm> as of July 18, 2011.
- Ohring, G., A. Gruber and R. G. Ellingson, 1984: Satellite determinations of the relationship between total longwave radiation flux and infrared window radiance. *J. climate & Appl. Meteor.*, **23**, 416-425.
- Turner, E. C., H.-T. Lee and S. F. B. Tett, 2015: Using IASI to simulate the total spectrum of outgoing long-wave radiances, *Atmos. Chem. Phys.*, **15**, 6561-6575, doi:10.5194/acp-15-6561-2015.
- Warner, J. X. and R. G. Ellingson, 2000: A new narrowband radiation model for water vapor absorption. *J. Atmos. Sci.*, **57**, 1481-1496.
- Wielicki, B. A., B. R. Barkstrom, E. F. Harrison, R. B. Lee, G. L. Smith, and J. E. Cooper, 1996: Clouds and the Earth's Radiant Energy System (CERES): An Earth Observing System Experiment. *Bull. Amer. Meteor. Soc.*, **77**, 853-868.
- Wong, T., B. A. Wielicki, R. B. Lee, III, G. L. Smith, K. A. Bush, and J. K. Willis, 2006: Re-examination of the Observed Decadal Variability of Earth Radiation Budget using Altitude-corrected ERBE/ERBS Nonscanner WFOV data. *J. Climate*.
- Young, D. F., P. Minnis, D. R. Doelling, G. G. Gibson and T. Wong, 1998: Temporal Interpolation Methods for the Clouds and the Earth's Radiant Energy System (CERES) Experiment. *J. Appl. Meteorology*, **37**, 572-590.

Appendix A. Acronyms and Abbreviations

Acronym or Abbreviation	Definition
ABI	Advanced Baseline Imager
AVHRR	Advanced Very High Resolution Radiometer
CATBD	Climate Algorithm Theoretical Basis Document
CDR	Climate Data Record
CERES	The Cloud and the Earth's Radiant Energy System
ECT	Equator Crossing Time
EOS	Earth Observing System
ERBE	Earth Radiation Budget Experiment
ERBS	Earth Radiation Budget Satellite
FOV	Field of View
GCOS	Global Climate Observing System
GERB	Geostationary Earth Radiation Budget Experiment
GOES	Geostationary Operational Environment Satellite
GSIP	GOES Surface and Insolation Product
HIRS	High-resolution Infrared Radiation Sounder
LUT	Lookup Table
LZA	Local Zenith Angle
MetOp	Meteorological Operational Polar Satellite
NASA	National Aeronautics and Space Administration
NESDIS	National Environmental Satellite, Data, and Information Service
NCDC	National Climatic Data Center
NOAA	National Oceanic and Atmospheres Administration
POES	Polar-orbiting Operational Environmental Satellite
RTM	Radiative Transfer Model
SDS	Scientific Data Sets
STD	Standard Deviation
TIROS	Television Infrared Observation Satellite
TOA	Top of Atmosphere
TOVS	TIROS Operational Vertical Sounder
WMO	World Meteorological Organization

Appendix B. Monthly OLR CDR v02r07 Revisions

The OLR retrieval algorithm has been modified for the v02r07 Monthly OLR CDR product. This section compares the old and new algorithms and describes the improvement.

v2.2 OLR retrieval algorithm (old) follows the formulation of Eq. 3.4, but uses different set of predictors for HIRS/2, 2i, 3 and 4 instruments. For HIRS/2, the prediction radiances are from channels 3, 7, 10 and 12 (Eq. B.1); while for HIRS/2i/3/4, they are from channels 3, 10, 11 and 12 (Eq. B.2).

$$OLR = a_0 + a_1 \cdot N_{ch3} + a_2 \cdot N_{ch7} + a_3 \cdot N_{ch10} + a_4 \cdot N_{ch12} \quad (B.1)$$

$$OLR = a_0 + a_1 \cdot N_{ch3} + a_2 \cdot N_{ch10} + a_3 \cdot N_{ch11} + a_4 \cdot N_{ch12} \quad (B.2)$$

Note that the dependence of local zenith angle in the regression coefficients and radiances was not shown in the expressions for brevity.

The change of regression models is necessary due to the unavailability of the lower tropospheric water vapor sensing channel (originally HIRS/2 Ch10) on HIRS/2i/3/4 instruments. (See Figure 14)

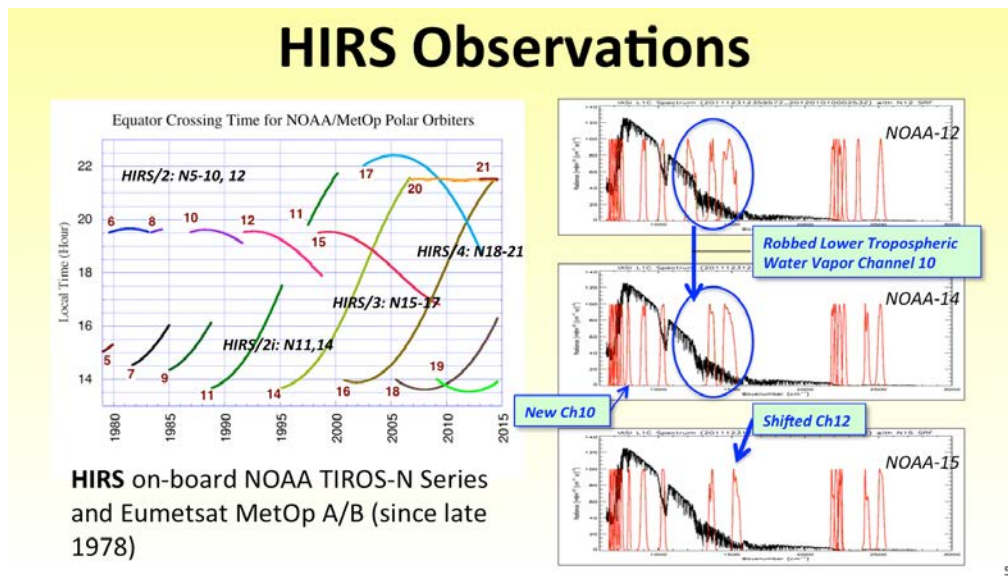


Figure 14 Description of HIRS instrument variations.

Although instantaneously the OLR retrieval maintain similar performances from either set of predictors, but the changed sensitivity to various parts of the atmospheric constituents and the earth surface produces scene-dependent differences that make the inter-satellite calibration difficult and very likely erroneous when sampling representativeness is at issue.

A new regression model formulation is determined to eliminate the instrument dependencies. An optimal set of common channels that are almost identical on all four

versions of HIRS instruments is formed. At the same time, non-linear predictors are introduced to secure endpoint performance.

$$OLR = a_0 + a_1 \cdot N_{ch3} + a_2 \cdot N_{ch7} + a_3 \cdot N_{ch8} + a_4 \cdot N_{ch11} + a_5 \cdot N_{ch8}^2 + a_6 \cdot \sqrt{N_{ch11}} + a_7 \cdot \sqrt{N_{ch12}} \quad (B.3)$$

The improvement in OLR retrieval consistency can be seen in the comparison of the regression residuals. When the retrievals from two instruments are consistent, they should produce “one-to-one” regression residuals distributions (consider each case is certain type of scene).

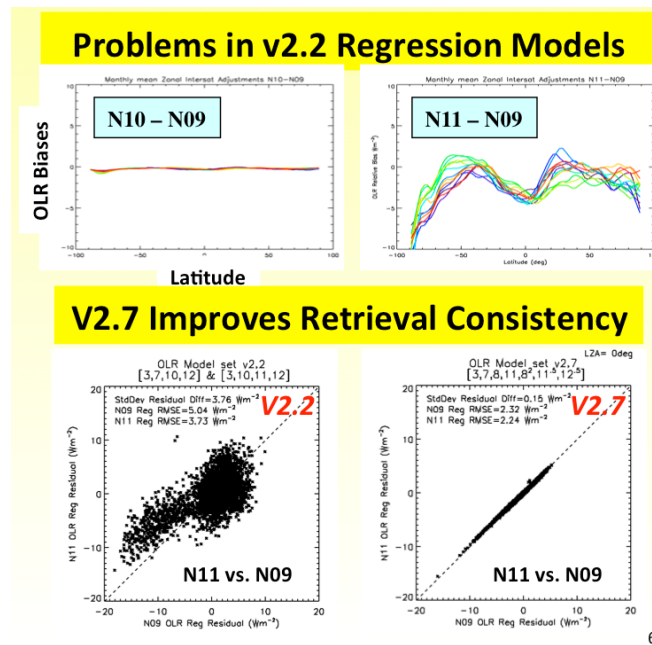


Figure 15 Illustration of consistency issues in OLR retrievals and the improvements made with new regression model.

Figure 15 illustrates the improvements of the retrieval consistencies. The inter-satellite biases between NOAA-10 and NOAA-9 using v2.2 retrieval algorithm (top left panel) are independent of latitude because both NOAA-10 and 9 are HIRS/2 instruments. But when comparing the retrievals between a HIRS/2 instrument (NOAA9) and a HIRS/2i instrument (NOAA11), their inter-satellite biases between show significant latitudinal dependence (top right panel) – resulted from the different sensitivity in the OLR regression models. Consequently, the retrieval residuals between NOAA11 and NOAA9 are not consistent (not in one-to-one relationship as shown in bottom left panel). When the retrievals were generated using the common set predictors (Eq. B.3) for NOAA11 and 9, their regression residuals show very good one-to-one relationship.

Figure 16 shows that the new OLR retrieval algorithm removed the artificial trend in the global OLR anomaly time series in v2.7 (cyan) without changing the tropical OLR anomalies. Note that the tropical OLR anomaly time series was the primary validation

parameter and has been compared well between the v2.2 Monthly CDR and other reference data sets.

Figure 17 shows the comparison of OLR CDR products against the CERES EBAF Ed2.6r product. The large amplitude in the “Monthly CDR v2.2 minus EBAF” differences (cyan) indicates disagreement in annual cycle. The agreement in annual cycle is improved in the Monthly CDR v2.7 (green) due to OLR retrieval algorithm revision. The remained differences in annual cycle between the Monthly CDR v2.7 and EBAF are caused by the diurnal variation estimation in v2.7. When the diurnal variation is explicitly accounted for, as in the Daily CDR v1.2 (red) that also uses the new OLR retrieval algorithm but aided with geostationary observations for temporal integral, the differences in annual cycles are minimized. (Note that the EBAF product also uses the geostationary observation for temporal integration purpose.)

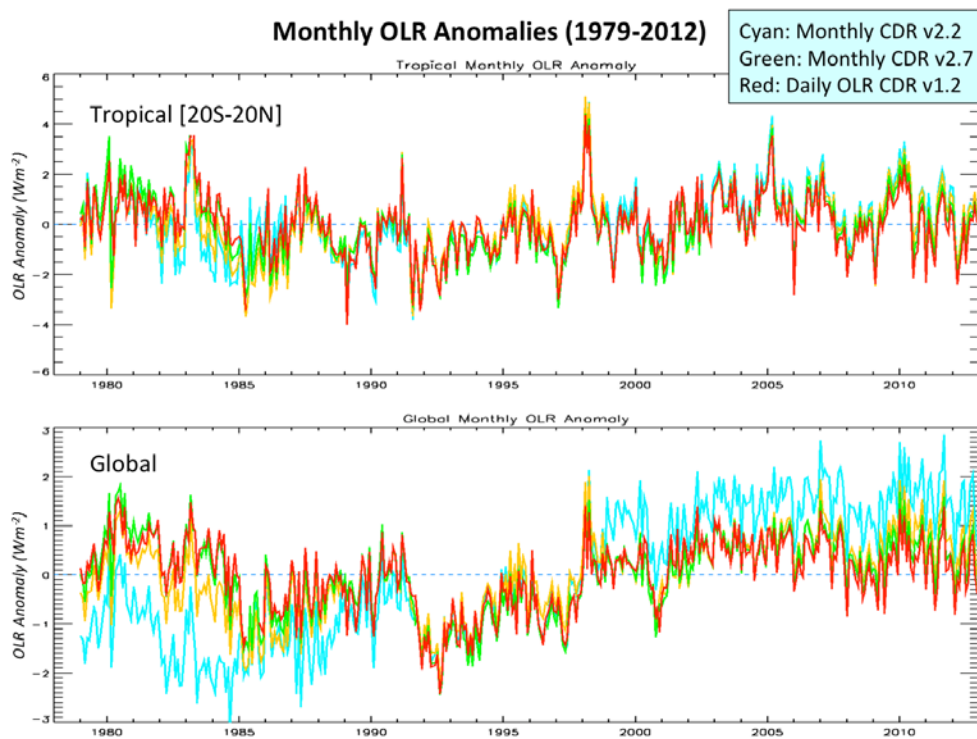


Figure 16 Comparison Tropical and Global OLR Anomalies of OLR CDR products (Monthly v2.2, v2.7 and Daily v1.2).

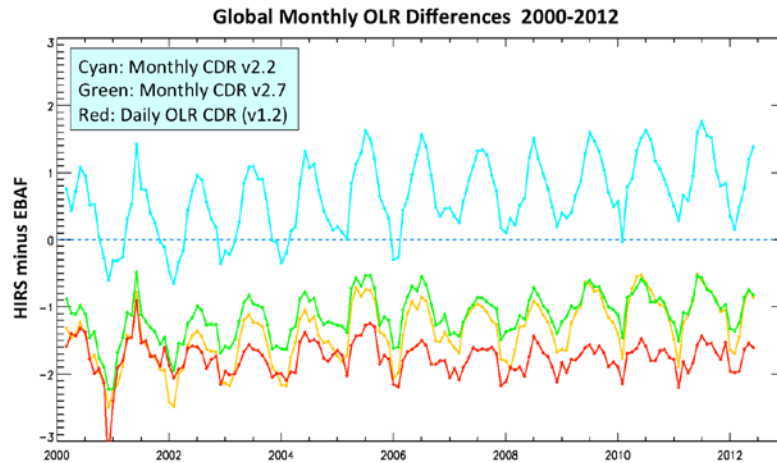


Figure 17 Comparison of OLR CDR (Monthly v2.2, v2.7 and Daily v1.2) products against CERES EBAF v2.6r OLR product.

Figure 18 compares the global OLR anomaly time series between the OLR CDR products and the Reanalysis data sets. It can be seen that the Monthly CDR v2.2 deviates from all other data sets, while the Daily CDR v1.2 tracks well with the reanalysis data sets. Note that the Daily CDR v1.2 is representative of the Monthly CDR v2.7 behavior because they use identical OLR retrieval algorithm and the same set of intersatellite calibration corrections.

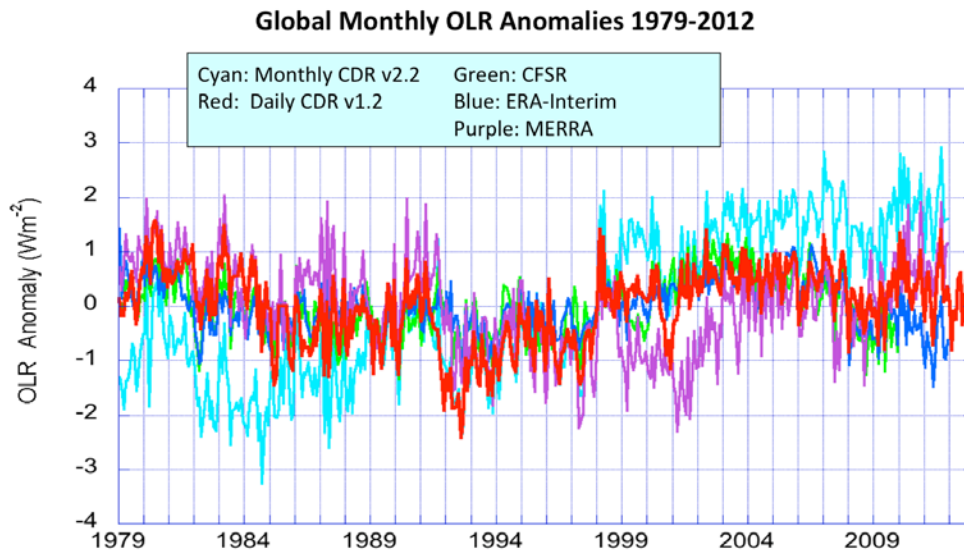


Figure 18 Comparison of OLR CDR (Monthly v2.2, and Daily v1.2) products with Reanalysis data sets, CFSR, ERA-Interim and MERRA.